

## Supplementary Information

# Excited state dynamics and generation of TTF radical cation inside a water-soluble nanocage

Sunandita Paul, Vamsee K. Voora and Jyotishman Dasgupta\*

Department of Chemical Sciences, 1 Homi Bhabha Road, Tata Institute of Fundamental  
Research, Mumbai 400005, India.

\*E-mail: [dasgupta@tifr.res.in](mailto:dasgupta@tifr.res.in)

1. Materials and Methods.....	3
2. Supplementary Figures.....	6-19
S1: NMR spectra of Pd <sub>6</sub> L <sub>4</sub> cavity	
S2: Comparison of absorption spectra of free guests with host-guest complex	
S3: Comparison of emission spectra of free guests with host-guest complex	
S4: Excitation spectra DiMeTTF inside cavity	
S5: Cyclic voltammetry of Guest molecules and host-guest complex.	
S6: Raman spectra of DiMeTTF⊂EnCage compared to free EnCage in water.	
S7: Computed Raman Spectra of TTF and TTF radical cation.	
S8: Kinetic decay from Global analysis of Transient Absorption data at 425 nm excitation.	
S9: Kinetic decay from Global analysis of Transient Absorption data at 615 nm excitation.	
S10: Residual of DiMeTTF⊂Enacge after SVD in a two-state sequential model.	
S11: Transient absorption of DiMeTTF in DCM at 350 nm excitation.	
S12: Planar structure of TTF radical cation in its D0 electronic state.	
S13: Bent structure of TTF radical cation in its D1 electronic state.	
S14: Planar structure of TTF radical cation in its D2 electronic state.	
S15: Twisted structure of TTF radical cation in its D2 electronic state.	
S16: Absorption spectra comparing steady state absorption and hot ground state absorption from transient spectra.	
S17: Comparison of the 63 picosecond component for free DiMeTTF with the long-lived residual	
S18: Computed transitions for TTF radical cation using TD-DFT	
Supporting Table 1 – 4 : Output details of DFT calculations	
3. References .....	20

## 1. Materials and Methods:

**Chemicals Used:** Tetrathiafulvalene and dimethyltetrathiafulvalene was purchased from Merck and TCI chemicals respectively. For synthesizing the nanocage PdCl<sub>2</sub>, ethylenediamine and AgNO<sub>3</sub> was bought from Merck chemicals. The triazine ligand of the cavity was bought from TCI chemicals and used as purchased.

**Sample preparation:** Solid EnCage powder was weighed and dissolved in water by stirring for 25 minutes at 60°C in oil bath to prepare a 2.5 mM solution. One molar equivalent of solid TTF or DiMeTTF powder was weighed and added to the EnCage solution, and stirred in dark for 2 hours in a glass vial at room temperature and ambient pressure. The solution was then syringe filtered to remove the excess solid TTF in solution. This was used for all further experiments.

**Synthesis of the cationic (Pd6L4) cage:** EnCage was prepared according to the reported literature by M. Fujita et al. *Nature*, 1995, 378, 469. A solution of Pd(En)(ONO<sub>2</sub>)<sub>2</sub> in H<sub>2</sub>O was taken to which 2,4,6-tri(4-pyridyl)-1,3,5-triazine was added in a molar ratio of 6:4. The suspension then stirred for 24 hrs and then heated at 80 C for 2 hrs. It was then filtered hot and washed with hot water<sup>1-2</sup>. The filtrate was then evaporated to dryness and a pale white powder was obtained. <sup>1</sup>H NMR was recorded for characterization (600MHz, D<sub>2</sub>O, 298 K): δ 9.00 (d, 24H, pyridine-α), 8.51 (d, 24H, pyridine-β), 2.85 (s, 24H) as shown in Figure S1.

**Steady State Optical Spectroscopy:** Steady state absorption measurements were carried out in JASCO V-670 spectrophotometer. All absorption measurements were done by appropriately diluting a 2.5 mM stock solution in a quartz cuvette of 1 mm pathlength. We used 250 μM concentration for absorption measurements of the empty EnCage cage in water and the free TTF solubilized in CH<sub>2</sub>Cl<sub>2</sub>. For the mixture that is the host-guest complex we used 2.5 mM of the complex with 1:1 host-guest stoichiometry.

All steady state emission measurements were done in Flourolog-3 (Horiba Jobin Yvon Inc) spectrofluorometer with Xe lamp as excitation source and PMT detector. Emission for TTF and DiMeTTF was taken in 1mm pathlength cuvette at 250 uM concentration in DCM keeping slitwidth of 5 nm. For the host guest complex 2.5 mM concentration was used in a 1mm pathlength cuvette.

**EPR Measurements:** Steady state EPR was recorded in X-band Bruker EMX 300 spectrometer. Recording of EPR was done by taking the sample in a quartz capillary of 2 mm diameter which was kept inside standard quartz EPR tube. The microwave frequency used was 9.3324 GHz. The data was recorded with a changing the magnetic field intensity with a center field of 3315 Gauss. A spectral width of 75 Gauss was taken with a resolution of 1024 data points in the X-axis and modulation amplitude of 1 Gauss. WinEPR Simfonia was used a software for data fitting the EPR data.

**Steady State Raman Measurements:** Steady state Resonance Raman measurements were done on Alpha 300R confocal Raman microscope of WITec GmbH, Ulm (Germany). The resonance excitation was done at 532 nm using a solid state frequency-doubled DPSS Nd:YAG laser. It is a confocal Raman setup where a 100  $\mu\text{m}$  optical fiber was used to collect the backscattered photons and then focused on a lens-based ultrahigh throughput spectrometer (UHTS300) with 1800 grooves/mm grating, which was coupled to a back-illuminated CCD camera ( $1024 \times 128$  pixels, Peltier-cooled to  $-65\text{ }^\circ\text{C}$ ) for detection. The spectral resolution achieved was  $\sim 2\text{ cm}^{-1}$ . To prevent degradation of sample, it was circulated in a flow quartz flow cuvette of 2 mm thickness on which the excitation laser was focused by a 10x lens.

**Cyclic Voltammetry Measurements:** Cyclic voltammetry measurements were done in a standard CH Instrument Spectro-electrochemical set up. Platinum electrodes were used both as working and counter electrode. The reference electrode was a standard Silver- Silver Chloride electrode. CV spectra of pure TTF and DiMeTTF in Acetonitrile was recorded with 0.1 M tetraethylammoniumtetrafluoroborate as electrolyte. The CV of the host guest complex in water was recorded with 5 mM  $\text{NaNO}_3$  as electrolyte.

**Femtosecond Transient Absorption Measurements:** Time resolved absorption measurements were done using femtosecond transient absorption setup which has been described in details previously<sup>3</sup>. A mode-locked femtosecond ( $\sim 10$  fs) pulse was generated using Ti-Sapphire crystal with bandwidth of  $\sim 100$  nm and  $\sim 400$  mW power at a repetition rate of 80 MHz (Coherent Micra-5 Mode-locked Ti:sapphire Laser system). It was then amplified using chirp pulse amplification in a commercial regenerative amplifier (Coherent Legend Elite Ultrafast Amplifier Laser system) to produce  $\sim 30$  fs pulses at 800 nm (65 nm bandwidth) with 3.5 W power and 1 KHz repetition rate. The output from the amplifier was directed at Coherent OPeraASolo Ultrafast Optical Parametric Amplifier system for

generation of 600 nm pump pulse. The power of the pump pulse was kept at ~500 nJ at sample stage for all measurements. A white light continuum was generated by focusing a small portion of the 800 nm pulse from the amplifier on a 2 mm thick sapphire crystal. This was used as a probe which was ~30 fs (420 nm- 1400 nm) in width. The pump was passed through a one-meter-long motorized translation stage outfitted with a quadra-pass mirror assembly delay stage for setting the time difference between the pump and probe. Both the pump and the probe were focused on the sample stage spatially and temporally. All measurements were carried out in a 1 mm flow cuvette connected to a peristaltic pump to circulate the liquid for avoiding any sample photodegradation. The IRF was ~100 fs for the measurements.

**Kinetic Data Fitting Procedure:** Single wavelength kinetic fits for transient absorption was fitted using multi-exponential decay constants in convolution with the respective instrument response function (IRF). It was done in Igor Pro5 Wavemetrics software to get the lifetime and amplitude of each decay component. The equation used was:

$$y = A_0 + \sum A_i e^{(-t/\tau_i)}$$

**Global Analysis of TA data:** Global analysis of the TA data was done using Glotran 1.5.1 software. Single value decomposition was done to obtain the Evolution associated spectra (EAS) and their corresponding lifetimes<sup>4</sup>.

**Theoretical studies:** All the computations used the uCAM-B3LYP functional and 6-311++g(d,p) basis sets. Gaussian 16 package<sup>5</sup> was used to run all the computations. The geometry optimization was carried out using the default SCF convergence criteria 1.00D-08 in convergence on RMS density matrix and 1.00D-06 in energy change. For all the optimized geometry both in ground state and excited state normal mode calculations were done and confirmed that there were no imaginary frequencies.

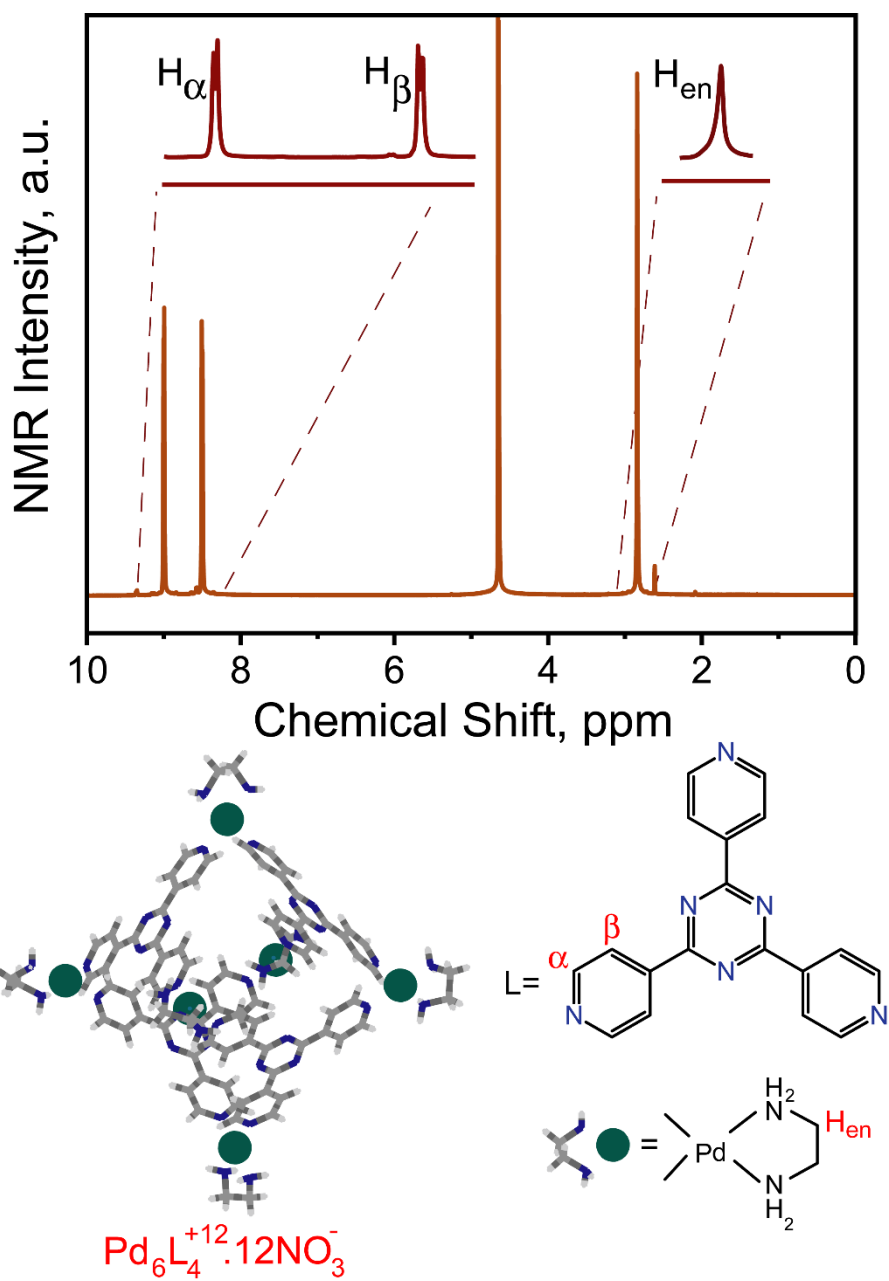


**Figure S1:** <sup>1</sup>H NMR spectrum (600 MHz, 298 K) of EnCage: δ 9.05 (d, 24H, pyridine-α), 8.51 (d, 24H, pyridine-β), 2.85 (s, 24H)

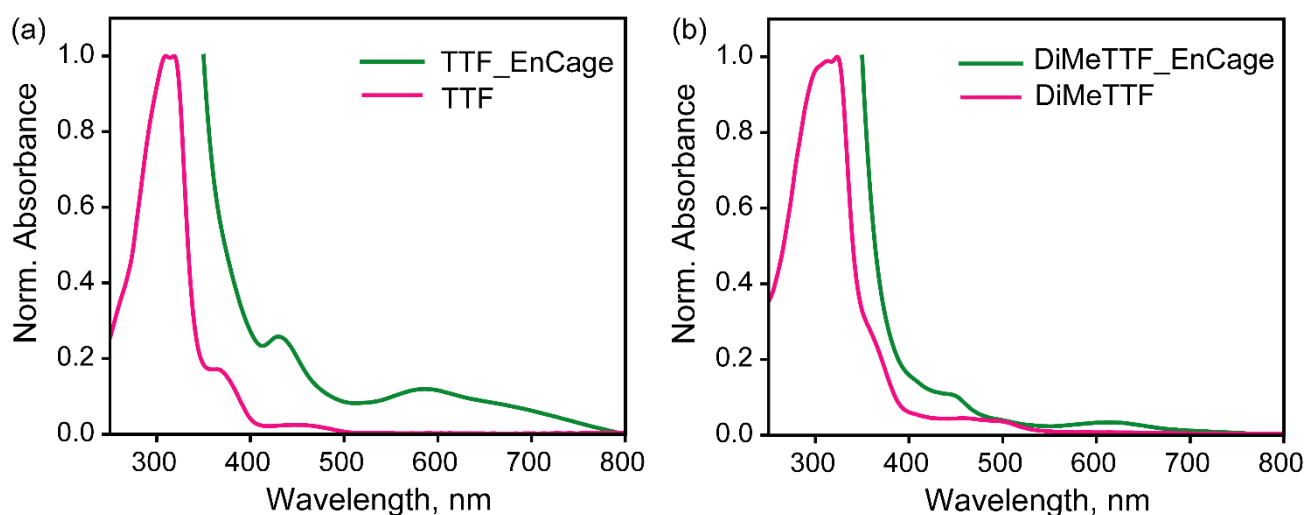


**Figure S2** (a): Comparison of absorption spectra of 250  $\mu\text{M}$  TTF in DCM with TTF inside Encage. (b) Comparison of absorption spectra of 250  $\mu\text{M}$  DiMeTTF in DCM with DiMeTTF inside Encage.

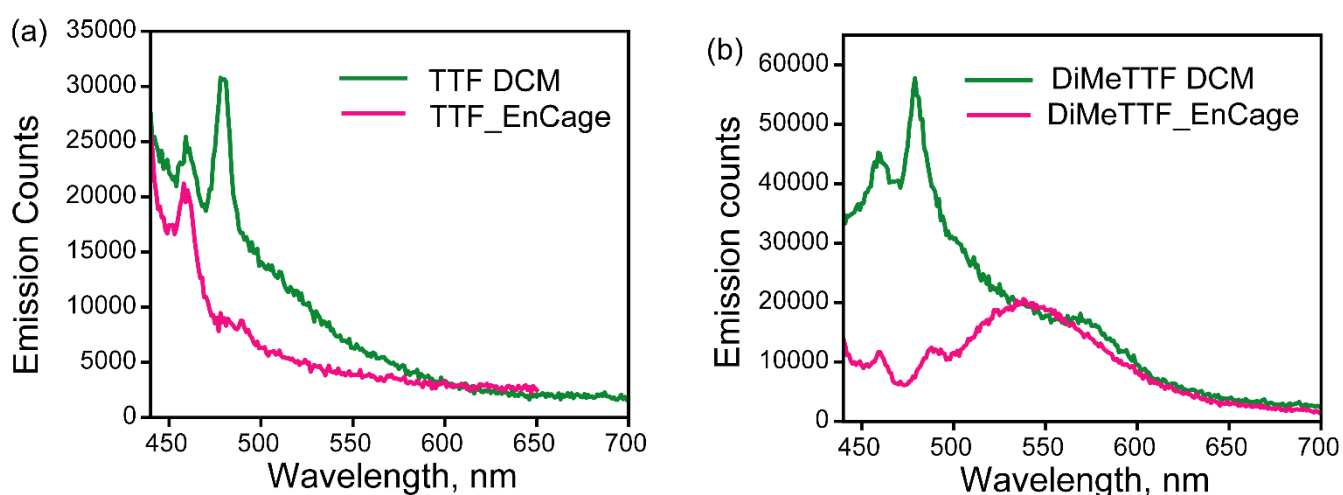


**Figure S3** (a): The green trace shows emission spectra of 250  $\mu\text{M}$  TTF in DCM at 420 nm excitation. The pink trace depicts emission spectra of 2.5 mM TTF $\subset$ Encage at 420 nm excitation. (b) The green trace shows emission spectra of 250  $\mu\text{M}$  DiMeTTF in DCM at 420 nm excitation. The pink trace depicts emission spectra of 2.5 mM DiMeTTF $\subset$ Encage at 420 nm excitation.

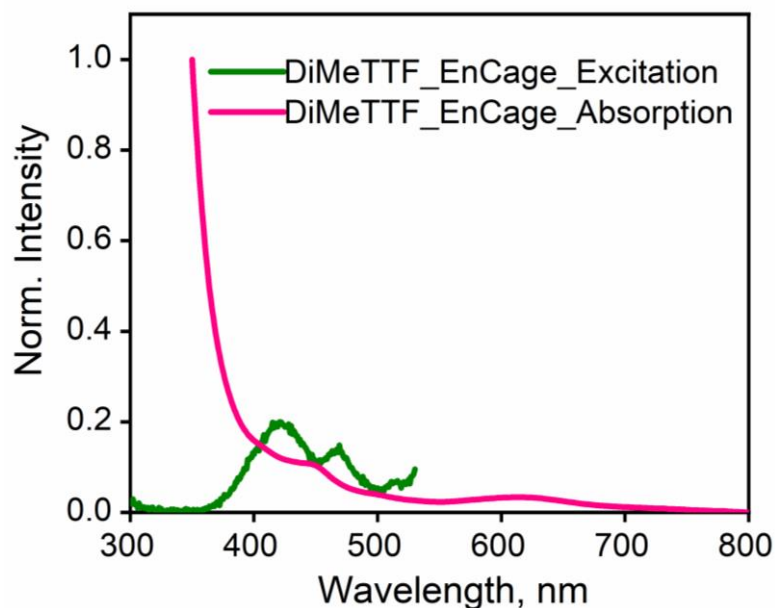


**Figure S4:** Excitation spectra of DiMeTTF⊂EnCage compared to absorption spectra of DiMeTTF⊂EnCage.

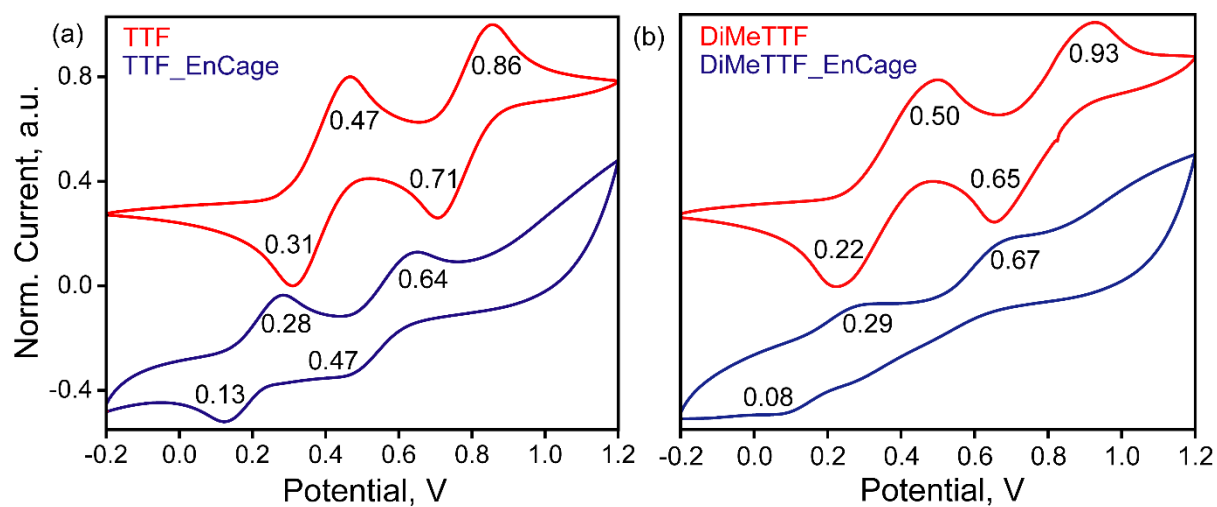


**Figure S5:** (a) Cyclic Voltammetry of neutral TTF in ACN (red) and TTF⊂EnCage in H<sub>2</sub>O. (b) Cyclic Voltammetry of neutral DiMeTTF in ACN (red) and DiMeTTF⊂EnCage in H<sub>2</sub>O. The clear shifts of the oxidation potentials to lower voltage signifies incarceration inside cavity.

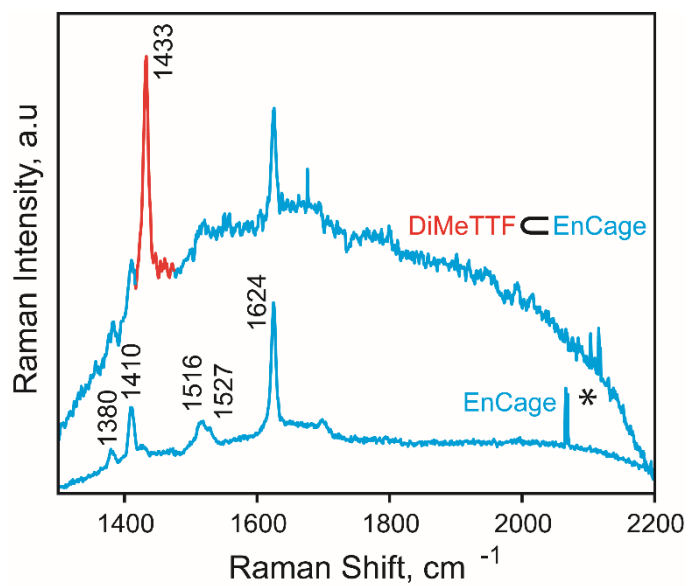


**Figure S6:** Resonance Raman spectrum of DiMeTTF  $\subset$  EnCage compared to Raman spectrum of empty cavity in water. Both the Raman spectra were recorded by 532 nm excitation. The peaks in the red shows vibrational features of DiMeTTF molecule inside the cavity.

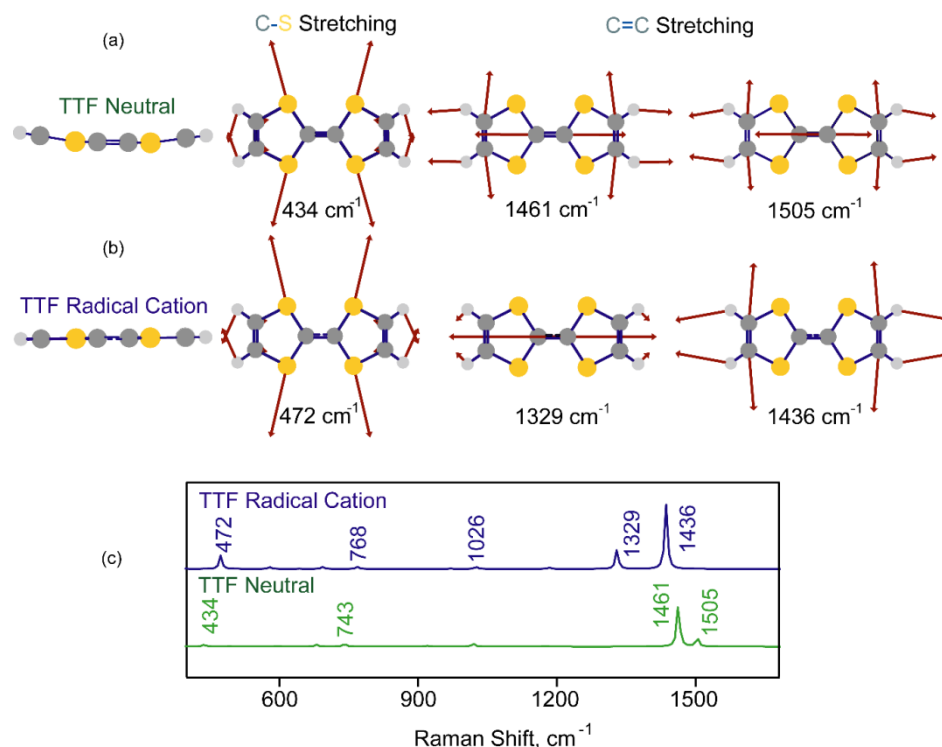


**Figure S7:** Computed Raman active modes of (a) Neutral TTF (b) TTF radical cation using DFT with uCAM-B3LYP functional and 6-311++g(d,p) basis set. The blue shift in C-S stretching mode and red shift in C=C bonds along with change in the displacement vectors of the C=C stretching modes in TTF radical cation matches with the expectation of structural and electronic changes in the radical cation formation. (c) The computed Raman modes in both Neutral TTF (blue) and TTF Radical cation (Green) are plotted against Raman Shift in cm<sup>-1</sup>.

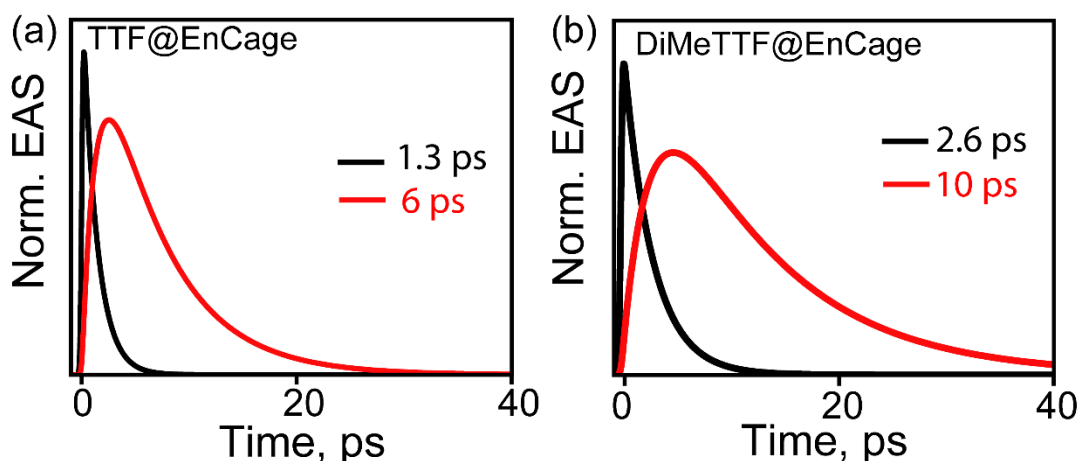


**Figure S8:** Population dynamics obtained subsequent to singular value decomposition (SVD) of the transient absorption data on 425 nm excitation from (a) TTF @ EnCage with two-state sequential decay model; and (b) DiMeTTF @ EnCage with two-state sequential decay model.

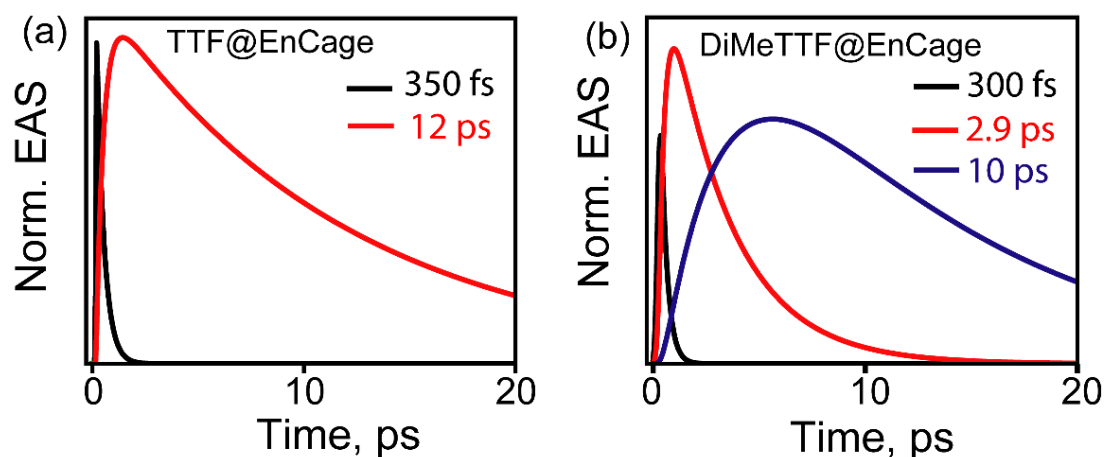


**Figure S9:** Population dynamics obtained subsequent to singular value decomposition (SVD) of the transient absorption data at 615 nm excitation from (a) TTF ⊂ EnCage with two-state sequential decay model; and (b) DiMeTTF ⊂ EnCage with three-state sequential decay model

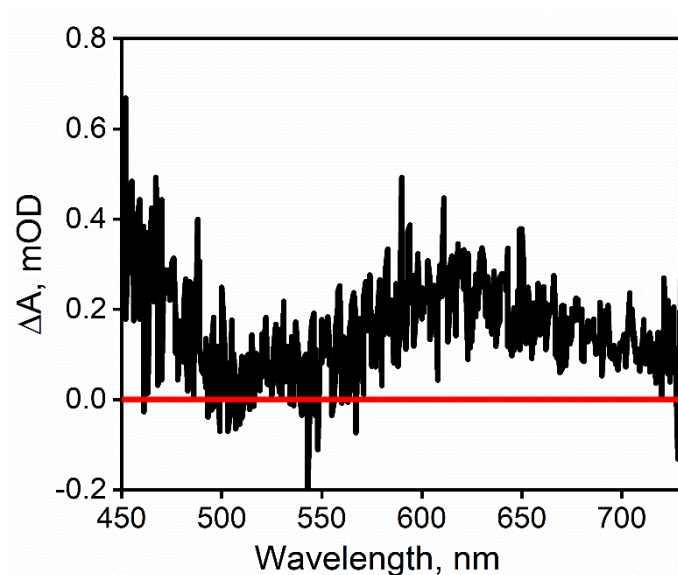


**Figure S10:** Residual at 1 ns of DiMeTTF ⊂ EnCage after singular value decomposition in a two-state sequential model.

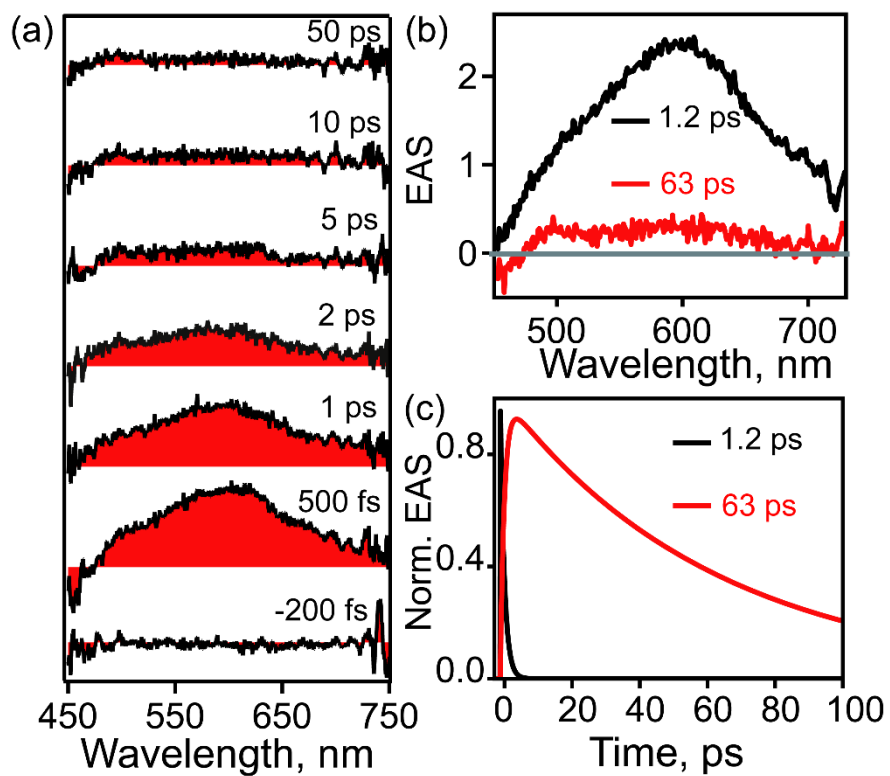


**Figure S11:** (a) Transient absorption of DiMeTTF in DCM (b) SVD showing a two state sequential decay with the respective lifetimes (c) Kinetics from SVD showing 2 state sequential model.

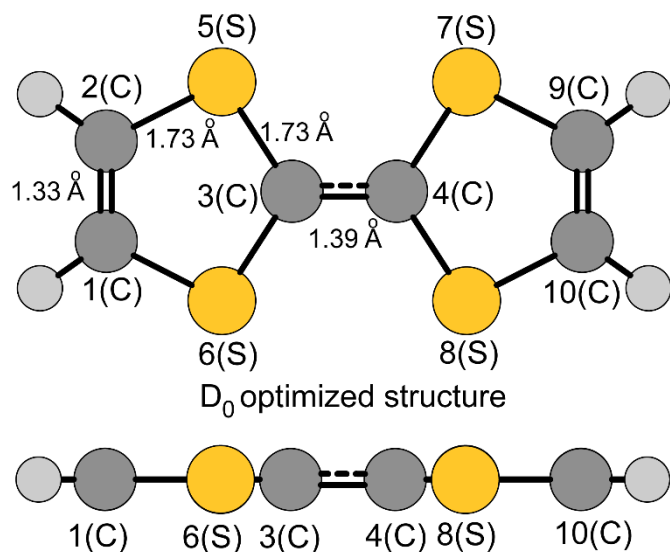


**Figure S12:** Planar structure of TTF radical cation in its D<sub>0</sub> electronic state and the representative bond lengths in Å<sup>o</sup> which was obtained using TD-DFT structure optimization at uCAMB3LYP/ 6-311++g(d,p) . The 5(S)-3(C)-4(C)-8(S) dihedral angle was 179.85°.

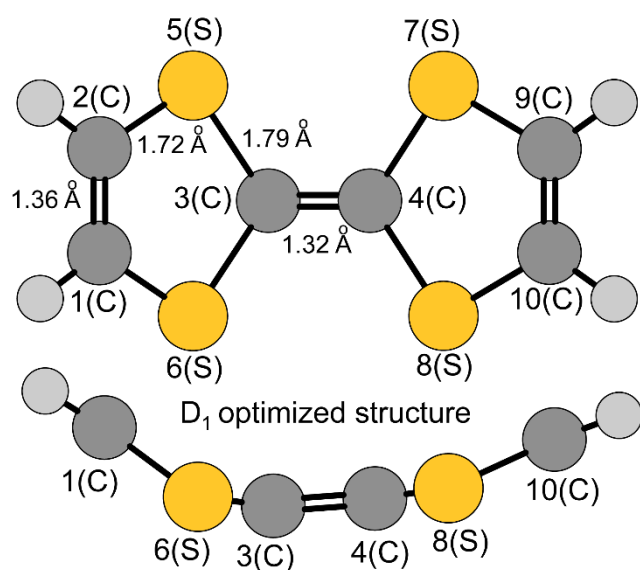


**Figure S13:** Bent structure of TTF radical cation in its D<sub>1</sub> electronic state and the representative bond lengths in Å<sup>o</sup> which was obtained using TD-DFT structure optimization at uCAMB3LYP/ 6-311++g(d,p). The 5(S)-3(C)-4(C)-8(S) dihedral angle was 170.40°. There is an asymmetry in the structure as shown. The dihedral angle between 6(S)-5(S)-3(C)-4(S) was 166.99° and 8(S)-7(S)-4(C)-3(S) was 175.4°.

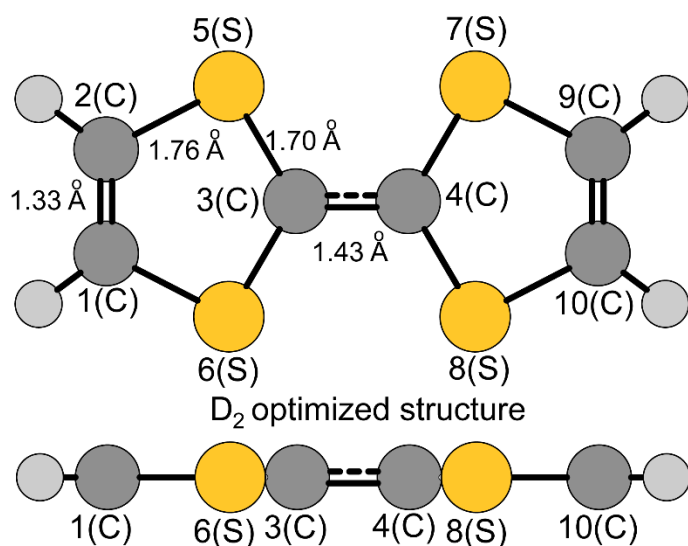


**Figure S14:** Planar structure of TTF radical cation in its D<sub>2</sub> electronic state and the representative bond lengths in Å° which was obtained using TD-DFT structure optimization at uCAMB3LYP/ 6-311++g(d,p). The 5(S)-3(C)-4(C)-8(S) dihedral angle was 179.94°.

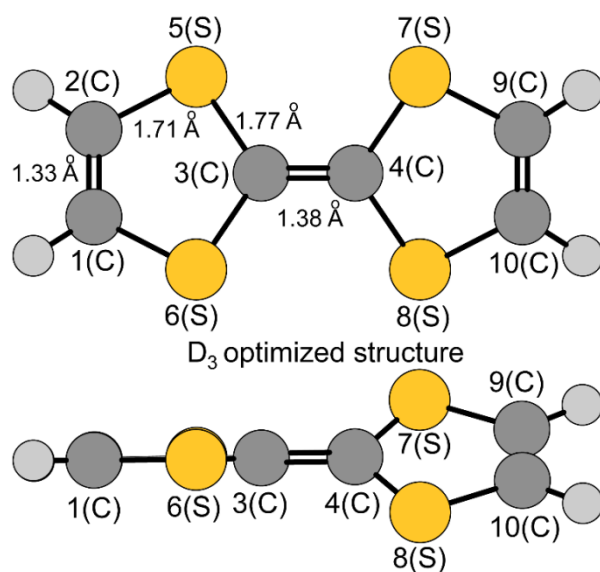


**Figure S15:** Planar structure of TTF radical cation in its D<sub>3</sub> electronic state and the representative bond lengths in Å° which was obtained using TD-DFT structure optimization at uCAMB3LYP/ 6-311++g(d,p). The 5(S)-3(C)-4(C)-8(S) dihedral angle was 146.56°.

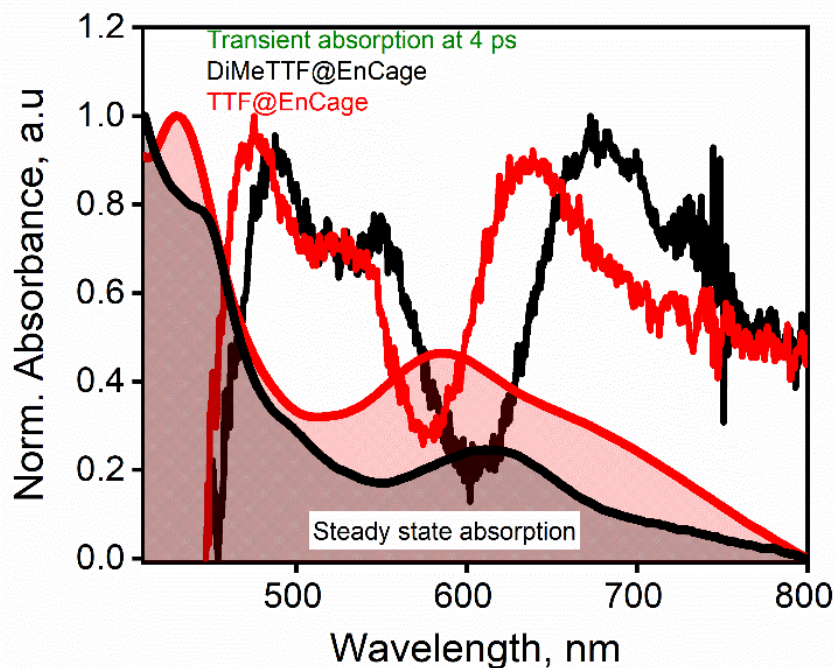


**Figure S16:** Steady state absorption of TTF@EnCage and DiMeTTF@EnCage has been compared to the transient absorption spectra obtained respectively for both the host-guest complexes at 4 ps. The red-filled spectrum shows ground state absorption of TTF@EnCage whereas the black-filled spectra show ground state absorption of DiMeTTF@EnCage. The red and black lined spectra show the transient absorption of TTF@EnCage and DiMeTTF@EnCage respectively at 4 ps indicating formation of hot ground state.

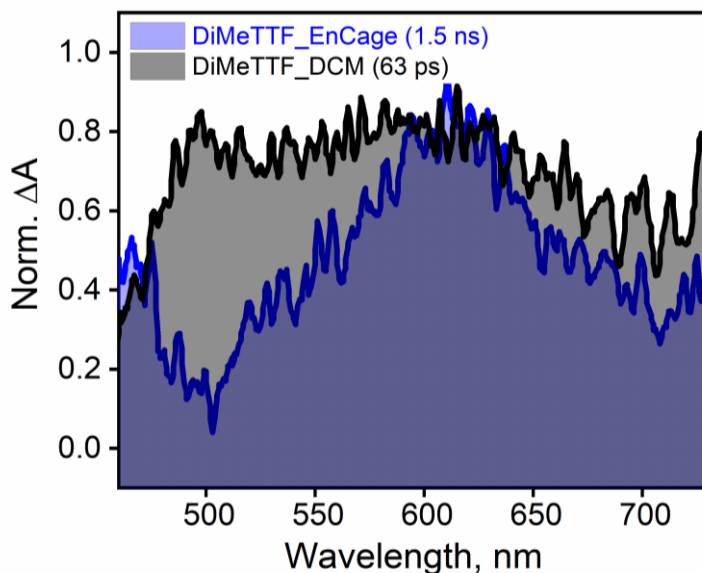


**Figure S17:** Comparison of the 63 ps lifetime component from transient absorption of DiMeTTF in DCM at 350 nm excitation to the long-lived residual from the transient absorption of DiMeTTF@EnCage. The  $\lambda$  max is seen at similar wavelength of 620 nm.

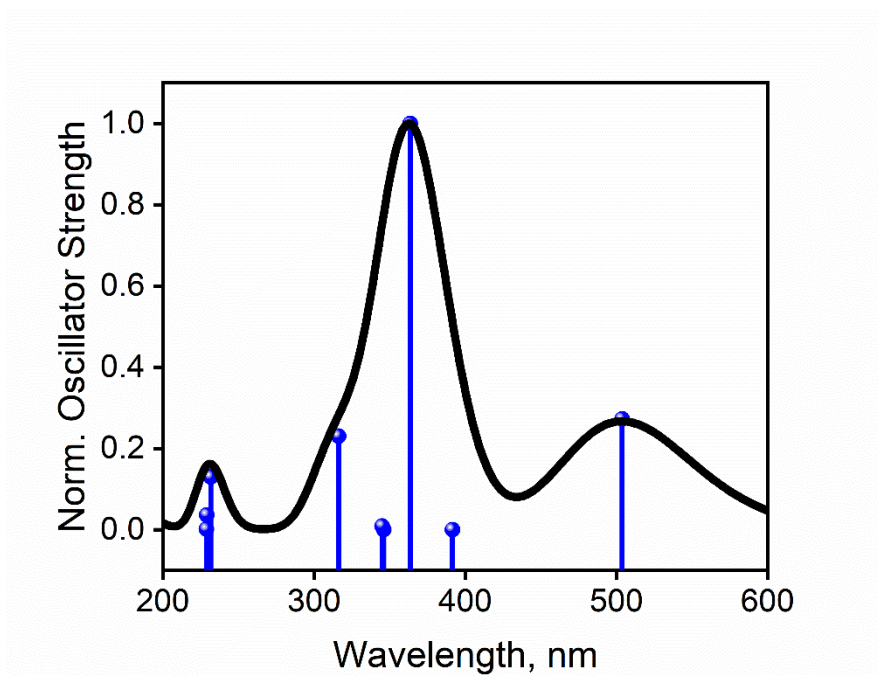


**Figure S18:** Computed transitions for TTF radical cation using TD-DFT with uCAMB3LYP/ 6-311++g(d,p). The stick spectrum in blue indicates the transition probabilities to higher excited state with respect to specific energy values as shown in wavelength scale. The black trace is the computed absorption spectra using a linewidth of 0.25 eV on the stick spectrum.

**Supporting Table 1:**TTF radical cation optimized geometry coordinates (D<sub>0</sub> optimized geometry)

Center Number	Atomic Number	Coordinates (Angstroms)		
		X	Y	Z
1	6	-3.171882	-0.667828	0.000628
2	6	-3.171801	0.667906	-0.000287
3	6	-0.696702	-0.000056	0.000275
4	6	0.696609	-0.000107	0.000447
5	16	-1.630511	1.456848	-0.001424
6	16	-1.630602	-1.456826	0.001207
7	16	1.630580	1.456795	0.001208
8	16	1.630610	-1.456832	-0.001477
9	6	3.171759	0.667847	0.000387
10	6	3.171816	-0.667754	-0.000245
11	1	-4.053670	1.293324	-0.000942
12	1	-4.053774	-1.293207	0.000673
13	1	4.053692	1.293153	0.001181
14	1	4.053740	-1.293069	-0.000355

**Supporting Table 2:**TTF radical cation optimized geometry in first excited doublet state (D<sub>1</sub> optimized geometry)

Center Number	Atomic Number	Coordinates (Angstroms)		
		X	Y	Z
1	6	-2.870196	-0.680847	0.638803
2	6	-2.870219	0.680807	0.638804
3	6	-0.674062	0.000025	-0.381172
4	6	0.648621	0.000036	-0.285012
5	16	-1.656559	1.501623	-0.264751
6	16	-1.656509	-1.501620	-0.264748
7	16	1.607163	1.496979	-0.150117
8	16	1.607119	-1.496965	-0.150141
9	6	2.983895	0.675539	0.482586
10	6	2.983873	-0.675585	0.482574
11	1	-3.642589	1.272801	1.113163
12	1	-3.642549	-1.272868	1.113158
13	1	3.827142	1.277341	0.795161
14	1	3.827105	-1.277413	0.795141

### **Supporting Table 3:**

TTF radical cation optimized geometry in third excited doublet state ( $D_3$  optimized geometry)

Center Number	Atomic Number	Coordinates (Angstroms)		
		X	Y	Z
1	6	-3.168101	-0.646529	0.197011
2	6	-3.168021	0.646860	-0.196365
3	6	-0.692921	-0.000207	-0.000280
4	6	0.692918	-0.000135	-0.000186
5	16	-1.654431	1.424740	-0.428363
6	16	-1.654647	-1.424940	0.427985
7	16	1.654324	1.424843	0.428199
8	16	1.654756	-1.424844	-0.428147
9	6	3.167965	0.646869	0.196884
10	6	3.168154	-0.646521	-0.196491
11	1	-4.065741	1.221286	-0.383679
12	1	-4.065915	-1.220651	0.384819
13	1	4.065640	1.221246	0.384571
14	1	4.066017	-1.220688	-0.383923

#### **Supporting Table 4:**

The TD-DFT oscillator strengths and the excitation energies computed using the optimized D<sub>0</sub> geometry of TTF radical.

	<u>Excitation energies</u>	<u>Oscillator strengths:</u>
Excited State 1:	2.4616 eV 503.68 nm	f=0.0849
Excited State 2:	3.1670 eV 391.49 nm	f=0.0001
Excited State 3:	3.4099 eV 363.60 nm	f=0.3119
Excited State 4:	3.5813 eV 346.20 nm	f=0.0000
Excited State 5:	3.5925 eV 345.12 nm	f=0.0028
Excited State 6:	3.7857 eV 327.51 nm	f=0.0000
Excited State 7:	3.9197 eV 316.31 nm	f=0.0717
Excited State 8:	4.3050 eV 288.00 nm	f=0.0000
Excited State 9:	4.4233 eV 280.30 nm	f=0.0000
Excited State 10:	4.5571 eV 272.07 nm	f=0.0000

## REFERENCES:

1. Fujita, M.; Oguro, D.; Miyazawa, M.; Oka, H.; Yamaguchi, K.; Ogura, K., Self-assembly of ten molecules into nanometre-sized organic host frameworks. *Nature* **1995**, *378*, 469-471.
2. Gera, R.; Das, A.; Jha, A.; Dasgupta, J., Light-induced proton-coupled electron transfer inside a nanocage. *Journal of the American Chemical Society* **2014**, *136*, 15909-15912.
3. Jha, A.; Chakraborty, D.; Srinivasan, V.; Dasgupta, J., Photoinduced charge transfer in solvated anthraquinones is facilitated by low-frequency ring deformations. *The Journal of Physical Chemistry B* **2013**, *117*, 12276-12285.
4. Snellenburg, J. J.; Laptanok, S. P.; Seger, R.; Mullen, K. M.; van Stokkum, I. H., Glotaran: A Java-based graphical user interface for the R package TIMP. **2012**.
5. Gaussian 16, Revision **C.01**, Frisch, M. J.; Trucks, G. W.; Schlegel, H. B.; Scuseria, G. E.; Robb, M. A.; Cheeseman, J. R.; Scalmani, G.; Barone, V.; Petersson, G. A.; Nakatsuji, H.; Li, X.; Caricato, M.; Marenich, A. V.; Bloino, J.; Janesko, B. G.; Gomperts, R.; Mennucci, B.; Hratchian, H. P.; Ortiz, J. V.; Izmaylov, A. F.; Sonnenberg, J. L.; Williams-Young, D.; Ding, F.; Lipparini, F.; Egidi, F.; Goings, J.; Peng, B.; Petrone, A.; Henderson, T.; Ranasinghe, D.; Zakrzewski, V. G.; Gao, J.; Rega, N.; Zheng, G.; Liang, W.; Hada, M.; Ehara, M.; Toyota, K.; Fukuda, R.; Hasegawa, J.; Ishida, M.; Nakajima, T.; Honda, Y.; Kitao, O.; Nakai, H.; Vreven, T.; Throssell, K.; Montgomery, J. A., Jr.; Peralta, J. E.; Ogliaro, F.; Bearpark, M. J.; Heyd, J. J.; Brothers, E. N.; Kudin, K. N.; Staroverov, V. N.; Keith, T. A.; Kobayashi, R.; Normand, J.; Raghavachari, K.; Rendell, A. P.; Burant, J. C.; Iyengar, S. S.; Tomasi, J.; Cossi, M.; Millam, J. M.; Klene, M.; Adamo, C.; Cammi, R.; Ochterski, J. W.; Martin, R. L.; Morokuma, K.; Farkas, O.; Foresman, J. B.; Fox, D. J. Gaussian, Inc., Wallingford CT, **2016**.